

ARTICLES

Multivalency of Sonic Hedgehog Conjugated to Linear Polymer Chains Modulates Protein Potency

Samuel T. Wall,^{†,||} Krishanu Saha,[§] Randolph S. Ashton,[§] Kimberly R. Kam,[‡] David V. Schaffer,^{†,§,||} and Kevin E. Healy^{*,†,‡,||}

Department of Bioengineering, Department of Materials Science and Engineering, Department of Chemical Engineering, and UCSF/UCB Joint Graduate Group in Bioengineering, University of California, Berkeley, California. Received July 15, 2007; Revised Manuscript Received February 6, 2008

A potentially active multivalent form of the protein Sonic hedgehog (Shh) was produced by bioconjugation of a modified recombinant form of Shh to the linear polymers poly(acrylic acid) (pAAc) and hyaluronic acid (HyA) via a two-step reaction exploiting carboimide and maleimide chemistry. Efficiency of the conjugation was ~75% even at stoichiometric ratios of 30 Shh molecules per linear HyA chain (i.e., 30:1 Shh/HyA). Bioactivity of the conjugates was tested via a cellular assay across a range of stoichiometric ratios of Shh molecules to HyA linear chains, which was varied from 0.6:1 Shh/HyA to 22:1 Shh/HyA. Results indicate that low conjugation ratios decrease Shh bioactivity and high ratios increase this activity beyond the potency of monomeric Shh, with approximately equal activity between monomeric soluble Shh and conjugated Shh at 7:1 Shh/HyA. In addition, high-ratio constructs increased angiogenesis determined by the *in vivo* chick chorioallantoic membrane (CAM) assay. These results are captured by a kinetic model of multiple interactions between the Shh/HyA conjugates and cell surface receptors resulting in higher cell signaling at lower bulk Shh concentrations.

INTRODUCTION

The use of chemical tethers to create solid-phase forms of biologically active agents is a recurring theme across a wide range of medical and biological applications. Chemical tethers can be used to attach bioactive peptide sequences or proteins to surfaces (1), to impart bioactivity to porous (2) or hydrogel implants (3, 4), or in a wide-ranging number of drug delivery applications (5–9). However, solid-phase presentation can potentially alter the way that such bioactive molecules work in a biological setting; cells interacting with tethered forms of ligands can have altered protein internalization for signal pathway activation (10), limited access of the ligands to appropriate cell surface receptors (11), and perturbed thermodynamics of receptor–ligand binding due to steric or avidity effects (12–14). As the dynamics of most growth factor responses are studied as single soluble molecular forms, it is important to understand how tethering molecules affects their potency and influences their use in biomedical applications, particularly for molecules whose natural forms are biologically tethered due to interactions with the extracellular matrix or cell surface lipid bilayers.

In this work, we describe a system for the attachment of recombinant proteins with added cysteine residues to long-chain

linear polymers containing free carboxylate groups, specifically the synthetic polymer poly(acrylic acid) (pAAc) and the biological polymer hyaluronic acid (HyA). This method, based on carboimide and maleimide chemistry, allowed for control of attachment stoichiometry of the large (~20 kDa) globular protein sonic hedgehog (Shh) to a long-chain linear polymer while maintaining protein activity. Progressively higher stoichiometric ratios of Shh to the linear polymer increased the potency of the protein by a factor of 10-fold over the soluble form as assessed by a cellular differentiation assay. In addition, the constructed multivalent proteins were tested for *in vivo* biological significance using an angiogenic assay utilizing the chick chorioallantoic membrane (CAM). In order to examine the mechanisms of increased activity of the multivalent form of the constructs, a kinetic model of the Shh pathway was developed to determine the likely effects of multiple binding events on the observed cellular response.

METHODS

Recombinant Shh and Bioconjugation Techniques. Using the cDNA of the N-terminal signaling domain of rat Shh (15), base pairs coding for an additional cysteine residue and a 6× His tag were added through PCR onto the c-terminus of the protein to allow for sulfhydryl-based reactions and protein purification, respectively. This tethering site was specifically chosen on the basis of studies demonstrating that this area of the protein is distant from its active site, and inert molecules attached there do not alter activity (16). In addition, two hydrophobic residues were added at the N-terminus to enhance the potency of the protein (18). The modified Shh PCR product was inserted into a pBAD-HisA (Invitrogen, Carlsbad, CA) plasmid, the resulting plasmid was confirmed by DNA sequenc-

* Correspondence to Professor Kevin E. Healy; University of California, Berkeley; 370 Hearst Memorial Mining Building, #1760; Berkeley, CA 94720-1760; E-mail: kehealy@berkeley.edu. Telephone: +510 643-3559. Fax: +(510) 642-5835.

[†] Department of Bioengineering.

[‡] Department of Materials Science and Engineering.

[§] Department of Chemical Engineering.

^{||} UCSF/UCB Joint Graduate Group in Bioengineering.

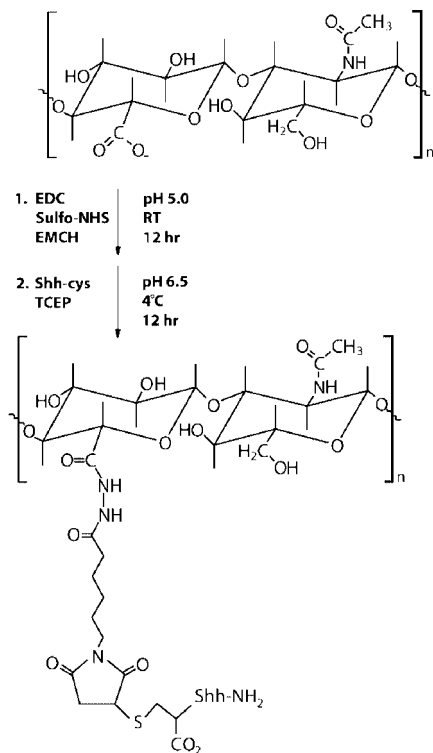


Figure 1. Bioconjugate scheme to graft recombinant Shh to the naturally derived polymer HyA (Shh-graft-HyA). A similar scheme utilizing the carboxylate groups on the polymer was used for the conjugation of the protein to synthetic high molecular weight poly(acrylic acid) (pAAc).

ing, and the protein expressed in BL21(DE3).pLys.E *E. coli* through arabinose induction. After induced protein expression, cells were lysed, and the resulting expressed Shh was purified using NiNTA (Qiagen, Valencia, CA) binding followed by imidazole elution. The purified protein was dialyzed into pH 7.4 PBS containing 10% glycerol, 2 mM EDTA, and 50 μ M ZnSO₄.

Purified Shh was conjugated to linear polymers through a two-step reaction using carbodiimide chemistry at the carboxylate group of the polymer and a maleimide reaction at the protein C-terminal cysteine (Figure 1). The first step was the addition of [*N*- ϵ -maleimidocaproic acid] hydrazide (EMCH, Pierce Biotechnology, Rockford, IL) to the linear polymer to allow for the subsequent attachment of the protein. This nonimmunogenic hydrazide–maleimide heterobifunctional cross-linker was added to the two linear polymers using the same general procedure, but with slightly different reaction conditions. For pAAc conjugates, 450 000 Da pAAc (Polysciences, Warrington, PA) at 2 mg/mL was reacted with 1-ethyl-3-[3-dimethylaminopropyl]carbodiimide hydrochloride (EDC) at 3.9 mg/mL, *N*-hydroxysulfosuccinimide (sulfo-NHS) at 1.1 mg/mL, and 0.5 mg/mL EMCH at room temperature for 2 h in pH 6.5 MES buffer as described for the attachment of small peptide sequences (17). For the activation of HyA, a method similar to that previously described for the attachment of hydrazides (9) was used with 10⁶ Da MW HyA (Genzyme, Cambridge, MA). This was dissolved and reacted at 3 mg/mL with the same concentrations of EDC, sulfo-NHS, and EMCH used in the pAAc reaction overnight in 0.1 M MES buffer, pH 5.0. After the attachment of the EMCH, the resulting maleimide-activated linear polymers were separated from the unconjugated reagents through sequential dilution and centrifugation in 50 000 MW cutoff centrifuge filters (Pall Gellman).

The activated polymers were then reacted with the Shh in varying stoichiometric feed ratios to produce conjugates of

varying molecular substitution. This reaction was performed at 4 °C overnight in 0.1 M MES buffer (pH 6.5) containing 50 μ M Tris(2-carboxyethyl)phosphine hydrochloride (TCEP, Pierce Biotechnology, Rockford, IL) to keep the C-terminus Shh cysteine reduced for duration of the reaction. After the reaction, any remaining maleimide groups on the linear polymer were reduced by the addition of 0.5 mM dithiothreitol and incubation at 4 °C for 1 h.

All conjugation reactions were assayed by gel electrophoresis, comparing reaction solutions to an equal mass of unreacted Shh to visually inspect protein coupling efficiency. In addition, sets of triplicate Shh/HyA conjugation reactions at 20:1 and 10:1 molar feed ratios of Shh to HyA were dialyzed overnight in 0.1 M MES buffer (pH 6.5) using Spectra/Por Float-A-Lyzer devices (Spectrum Laboratories, Rancho Dominguez, CA) to remove nonconjugated Shh. Protein concentrations in the dialyzed HyA-Shh solutions were then quantified using a microBCA assay (Pierce Biotechnology, Rockford, IL).

Bioactivity Assay. In order to test bioactivity, murine embryonic C3H10T1/2 cells (American Type Culture Collection, Manassas VA) were induced to differentiate into an osteogenic line by exposure to Shh as described elsewhere (18, 19). Briefly, the cells were plated at 5000 cells/well in 96 well plates in normal growth media (α MEM with 10% FBS). After 2 days, the medium was replaced with a low FBS (2%) media and supplemented with the proteins and/or conjugate reaction solutions. Test conditions included soluble Shh in the range of 1–100 nM, soluble Shh in the same range along with unconjugated HyA at 50 μ M, or the Shh/HyA conjugate in quantities such that the concentrations of Shh in the media solutions were also 1–100 nM. After incubation for an additional 3 days, the cells were washed and lysed, and the cell lysate was assayed for differentiation by measuring alkaline phosphatase (ALP) activity using the fluorescent probe 9-*H*-(1,3-dichloro-9,9-dimethylacridin-2-one-7-yl) phosphate (DDAO, Molecular Probes, Eugene OR). Unconjugated poly(acrylic acid) was shown to inhibit the differentiation of the cells, so bioactivity testing of these conjugates was not performed.

Angiogenesis Assay. As Shh is a known angiogenic agent (20), induced angiogenesis from soluble Shh and Shh/HyA conjugates was assayed using a CAM window assay. Fertile white leghorn eggs (Charles River, Franklin, CT) were incubated at 37 °C in a humidified environment until day 8, at which time 2 mL of albumin was removed from the blunt end of the egg, and a small 1 cm \times 1 cm window was made in the shell on the opposite side. Sterile squares of filter paper loaded with sterile PBS, 0.1 μ g of Shh, or 0.1 μ g Shh of the 20:1 Shh/HyA feed ratio conjugate were placed directly on the developing CAM. This window was then sealed with parafilm and the eggs returned to the incubator. Angiogenesis around the test materials was microscopically evaluated 3 days later using an Olympus SZX7 stereoscope. High-resolution photomicrographs were taken using an attached QImaging Qfire camera. These images were analyzed using *ImageJ* software to quantify the number of blood vessels per unit length in a square perimeter surrounding the implants at distances of 0.1 and 0.25 cm away from its edge. Linear density measurements for each group were tested for statistical significance using a one-way ANOVA on both the 0.1 and 0.25 cm distance data, followed by pairwise Holm's *t* tests of the individual groups.

Molecular Modeling of Shh–HyA Conjugate Cell Signaling. We built upon binding and trafficking numerical models that describe expression of Gli transcriptional effectors in response to monomeric Shh (21, 22) and numerical kinetic models describing multivalent ligand–receptor binding (Figure S1, Supporting Information) (23). To develop the simplest model for the C3H10T1/2 bioactivity data in Figure 3, the following

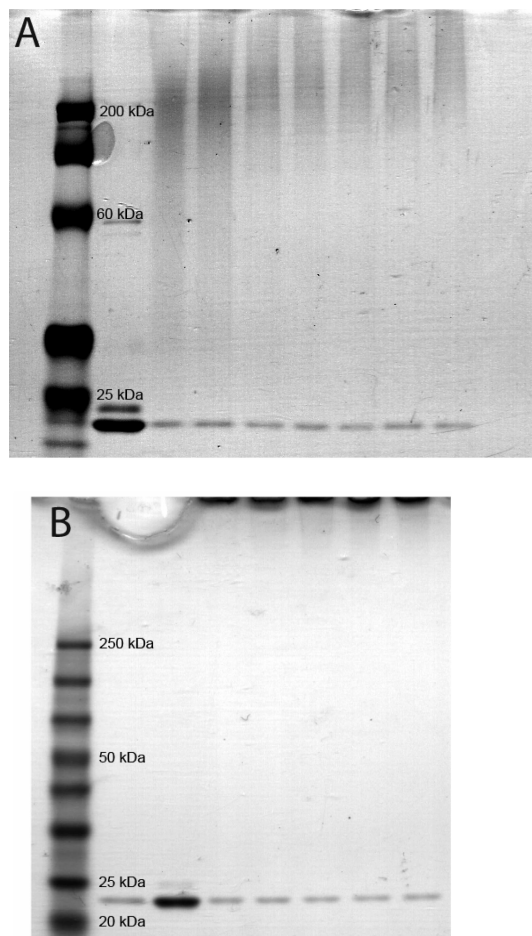


Figure 2. Gel electrophoresis of Shh and its conjugation products with pAAc (A) and HyA (B). In A, conjugates from 1:1 to 30:1 Shh/pAAc molar feed ratios appear as the loss of the Shh band and the appearance of a high molecular weight smear. In B, the large HyA conjugates are unable to enter the gel and are seen as bands residing at the top of the gel.

assumptions were invoked: Patched (Ptc) repression of Smoothed is not affected by the Ptc receptor aggregation; ligand-induced internalization rate is the same for all valencies; alkaline phosphatase activity is linearly proportional to Gli1 levels in a cell; and differentiation of a C3H10T1/2 cell does not change its responsiveness to Shh. Initial binding of the HyA–Shh conjugate was assumed to follow monomeric Shh–Ptc binding rates, but all other additional binding of Shh moieties from the conjugate to other Ptc receptors were assumed to occur at a higher rate. This assumption has been called the *equivalent site hypothesis* in that after initial binding, all subsequent sites on a multivalent conjugate for ligand binding are identical (24).

Model parameters were taken from literature (21, 22); however, a number of parameters were estimated directly from the bioactivity data in Figure 3. First, the monomeric Shh–Ptc binding constant k_{on}/k_{off} and the alkaline phosphatase activity/Gli1 expression ratio were estimated from the soluble Shh bioactivity curve. In addition, the multimeric Shh–Ptc binding constant was directly estimated from the 22:1 conjugate curve (see Table S1, Supporting Information). We also formulated an alternative model that incorporates steric hindrance of HyA chains as a simple reduction in conjugate binding affinity to Ptc. For the alternative model incorporating sterics, termed the “model with sterics”, the multimeric Shh–Ptc binding constant

Table 1. Conjugation Ratios and Coupling Efficiencies Determined for Shh/HyA Reactions at 30:1 and 10:1 Molar Feed Ratios

	molar ratio of Shh/HyA		percent coupling	
feed ratio	30:1	10:1	30:1	10:1
trial 1	21.80	6.91	73.3%	69.8%
trial 2	22.58	6.65	76.0%	67.1%
trial 3	22.09	7.02	74.3%	70.8%
average	22.16	6.86	74.5%	69.2%
stdev	0.40	0.19	1.3%	1.9%

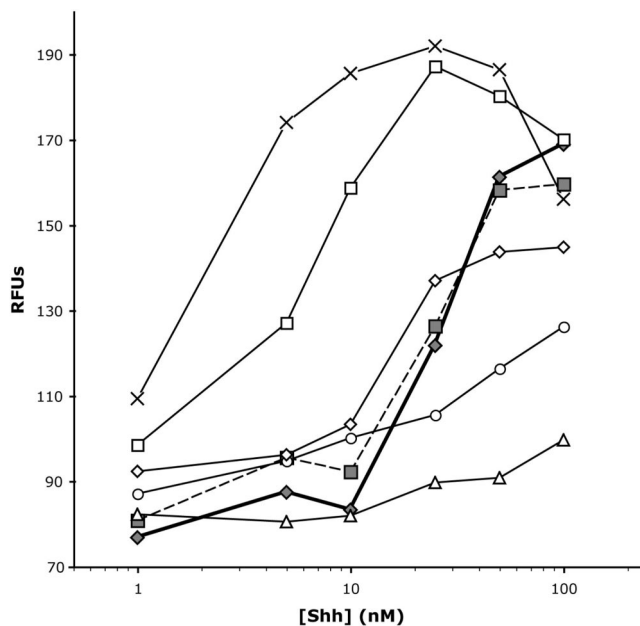


Figure 3. C3H10T1/2 bioactivity results against soluble Shh (◆, heavy line), soluble Shh with soluble HyA (■, dashed lines), and the Shh–HyA conjugates in stoichiometric ratios of 0.6:1 (△), 3.5:1 (○), 7:1 (◇), 14:1 (□), and 22:1 (×). Produced conjugates with Shh/HyA ratios of 0.6:1 and 3.5:1 have decreased efficacy on a unit basis of Shh compared to the freely soluble form, while 7:1–22:1 have increased bioactivity.

k_{on} for 0.6:1, 3.5:1, and 7:1 conjugation feed ratios was reduced 5.5-fold to match the experimental data from the 0.6:1 curve in Figure 3.

RESULTS

Chemical Conjugation. A recombinant rat Shh variant with a cysteine residue near the C-terminus was constructed, expressed, and purified via immobilized metal affinity chromatography. Conjugation of the recombinant protein was achieved on both pAAc and HyA with high efficiency. Using gel electrophoresis, it was apparent that the reaction produced a decrease in the monomeric Shh band (Figure 2) and the appearance of a high molecular weight conjugate. For pAAc (Figure 2A) (MW = 450 000), this produced a smear through the gel with an increasing mass as the Shh conjugation molar feed ratio increased from 1:1 to 30:1. For HyA (MW = 10^6 Da), the high molecular weight conjugates did not penetrate deeply into the gel. By contrast, simply mixing the Shh with raw pAAc or HyA did not alter the Shh mobility in the gel (data not shown). Protein analysis of purified Shh/HyA reactions at 10:1 and 30:1 molar feed ratios performed in triplicate indicated that the reaction was reproducible with a high degree of efficiency at approximately 70–75% (Table 1). Molar feed ratios of 1:1, 5:1, 10:1, 20:1, and 30:1 produced Shh–HyA conjugates with molar substitution ratios of 0.6:1, 3.5:1, 7:1, 14:1, and 22:1, respectively.

C3H10T1/2 Cell Bioactivity Assay. Through the use of the murine embryonic cell line C3H10T1/2, conjugation of the Shh

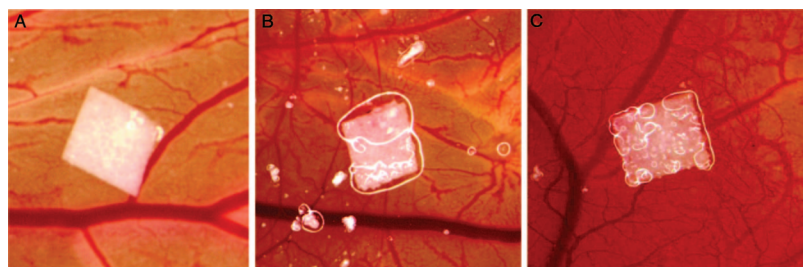


Figure 4. Panel of photomicrographs depicting CAM reactions to negative control samples (A), freely soluble Shh (B), and the 14:1 Shh/HyA multivalent form. Noted increased vessel density is apparent around the Shh sample as well as the conjugated form.

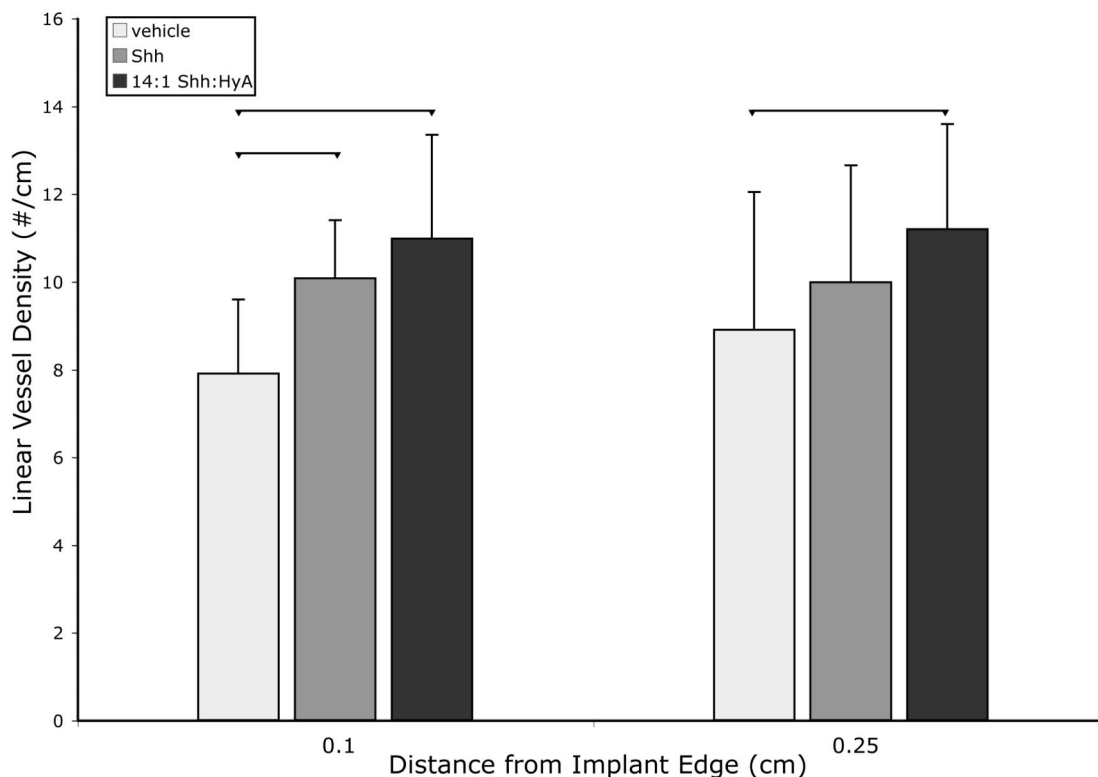


Figure 5. Quantitative results of angiogenesis in the CAM assay derived from photomicrograph image analysis. Increased vascular density is measured for both the soluble Shh and the Shh-graft-HyA in the 14:1 ratio. All three groups can be statistically separated at a distance of 0.1 cm from the edge of the implant, while at 0.25 cm, only the conjugated form is statistically different from the negative control.

was shown to dramatically alter the activity of the tethered protein when evaluated against actual Shh concentration in solution (Figure 3). Only HyA-conjugated Shh could be tested using this cell line, as pAAc inhibited the differentiation that soluble Shh induces in the cell line (data not shown). At low tethering (e.g., 3.5:1), the activity was decreased, with an estimated 10-fold increase in EC_{50} of the Shh in solution, presumably due to steric hindrances that the large linear polymer caused when attached. The activity increased back to normal when the conjugation ratio reached 7:1. Beyond this, activity of the tethered Shh was increased dramatically, with a 10-fold decrease in estimated EC_{50} values from the untethered Shh to the 22:1 construct.

CAM Angiogenesis Model. The CAM results indicated an increased potency for the conjugated Shh/HyA. Photographic analysis and quantification (Figures 4 and 5) revealed a statistically significant increase in vasculature around the Shh-loaded samples compared to the negative control within a close distance (0.1 cm) of the implant. While the Shh/HyA conjugated at a 14:1 ratio had an increased average vessel number over both the negative control and unconjugated Shh at 0.1 cm, it also had a longer-range persistent increase over the negative control at 0.25 cm. Although the soluble Shh also had an

increased average vessel number over the negative control at this distance, this observation was not statistically significant.

Numerical Modeling of Multivalent Shh Bioactivity. We developed simple kinetic models of HyA–Shh conjugate binding, trafficking, and downstream signal activation. To focus on the effects of conjugate multivalency, a number of assumptions were invoked in the simplified models: Ptc receptor aggregation does not affect signal transduction; ligand internalization is not affected by valency; alkaline phosphatase activity is linearly proportional to Gli1 levels in a cell regardless of differentiation; and only two rates of conjugate binding occur—an initial binding of the conjugate and a higher binding rate for all additional Shh moieties from the conjugate to other Ptc receptors (see Supporting Information for model equations and parameters). With these assumptions, two types of models were developed, one incorporating steric hindrance of HyA chains as a simple reduction in conjugate binding affinity to Ptc, and one neglecting any influence of steric hindrance. These two models were termed “model with sterics” and “model without sterics”, respectively. Under these assumptions, modeling results indicated that increasing the conjugation ratio of Shh to its HyA carrier in the bioactivity assay should result in a progressive increase in cell signaling and decrease in the EC_{50}

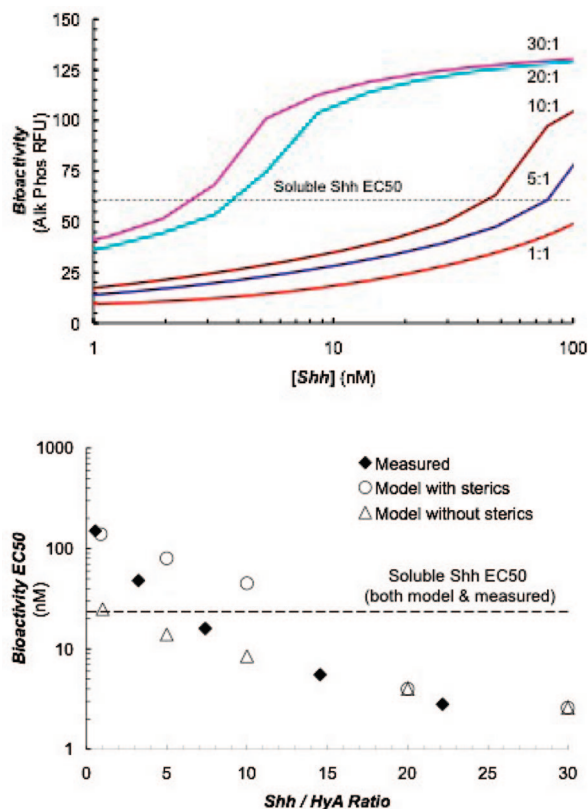


Figure 6. Numerical model results of Shh–HyA conjugate bioactivity in C3H10T1/2 cells. Activity as a function of Shh concentration for stoichiometric ratios 1:1–30:1 is shown on top for a model incorporating steric interaction (see text). A plot of EC_{50} versus substitution level for two types of models versus experimental results in Figure 3 is shown on the bottom. Both models capture the trend in EC_{50} with substitution ratio but fail to capture the increased amplitude of bioactivity for the 14:1 and 22:1 conjugates (see Figure 3).

(Figure 6). The estimated EC_{50} values from the experimental data were well-matched using both types of kinetic models at the tested conjugation ratios and with the aforementioned assumptions ($R^2 = 0.7$ for the model without sterics; $R^2 = 0.8$ for the model with sterics). For the model without sterics, EC_{50} values matched experimental results well at high conjugation ratios, but the modeling results overestimated the EC_{50} values for conjugation ratios 7:1 and lower (Figure 6). Results from the model with sterics can correct for this deviation (Figure 6); however, the fits at 3.5:1 and 7:1 conjugation ratios suggest that the exact mechanism of steric hindrance may vary from the one postulated in our model with sterics (see Discussion). Some features, such as the shape of the dose–response curve, as well as decreased peak location, were not as fit well using the developed model, as indicated by the comparison of Figures 3 and 6.

DISCUSSION

These results indicate that large proteins can be coupled to a linear polymer with high efficiency and controlled stoichiometry through the use of a heterobifunctional cross-linker under conditions that do not lead to loss of protein activity. On the contrary, coupling of a protein to a superstructure such as large linear polymer offers a method of modulating the activity of a protein by controlling its interaction with the cell. This method could be used to add multivalent protein functionality to both synthetic and biological polymers with equal efficiency. However, control of the reaction was much more difficult with the HyA than the pAAc. Conjugation to the pAAc was robust across

a wide range of reaction pHs, concentrations, and times. On the other hand, adding the EMCH to the HyA required considerable optimization of the reaction conditions, as the reaction was much more sensitive to pH, concentrations, and time. High overall coupling efficiencies were observed only in the mildly acidic pH range 5.0–5.5 for the attachment of EMCH to HyA, which was consistent with the work of Pouyani et al. (9) and Vercruyse et al. (25). At neutral pH, although there are successful reports of EDC/sulfo-NHS mediated HyA bioconjugation (26, 27) in these studies the overall conjugation was minimal. This may be due to hydrolysis of the maleimide rather than the lack of conjugation of the EMCH to the HyA chains, as the maleimide is susceptible to hydrolysis at pH > 6.5 and our scheme required long reaction times for the final protein attachment.

While the use of lower molecular weight HyA (~250 kDa) in hydrazide mediated bioconjugation is observed in the literature (28–30), reporting better handling and more reproducible conjugation results, in our studies we chose to use high molecular weight HyA in order to maximize spacing and flexibility between conjugated protein molecules. We obtained reproducible results using this material, with repeated conjugation reactions producing nearly identical conjugation efficiencies and bioactivity curves. However, these results may be contributable to the reaction scheme used, for in our synthesis, the reaction was limited by the amount of protein added to the reaction. As only ~1% of the available reaction sites on the HyA backbone are utilized on the highest conjugation ratio synthesized, if there is variability in the amount of EMCH substituted onto the backbone, this will be largely unnoticed as long as EMCH substitution rates exceed this small fraction of used sites.

The most striking result of our conjugation experiments was how the controlled attachment of Shh modulated protein activity as a function of valency. There are multiple possible mechanisms by which this increase in activity may result from tethering and include higher overall ligand affinity due to avidity effects, forced receptor multimerization, inhibition of receptor–ligand internalization, and changes to protein stability in solution. Such mechanisms have been previously identified and described for ligands such as DNA complexes (6, 7), protein inhibitors (8, 12), and growth factor pathways (10). We believe that similar mechanisms may be in action here, such as avidity effects from the interaction of multiple Shh molecules in the multivalent form with the Shh cell surface receptor Patched. Other mechanisms may be at play, as multimerization of Shh is known to change its short- and long-range activity in vivo (31), and internalization also plays a role in Shh activity (32, 33).

Using novel numerical models, we attempted to elucidate the mechanism by which the bioactivity changes upon conjugation. In comparison to monomeric soluble Shh, multivalent Shh–HyA conjugates may have altered trafficking, binding, degradation, and signaling. Ordinary differential equations provide a convenient means to track the kinetics of each of these processes during Shh signal transduction. Both models—one incorporating sterics and one without sterics—can recapitulate the EC_{50} decrease with increasing valency (Figure 6). The poor fit at 3.5:1 and 7:1 conjugation ratios is likely due to the simple mechanism of steric hindrance that we incorporated into our model. In particular, steric hindrance effects on conjugate binding to Ptc is likely to change with conjugation ratio, since the average HyA chain length between Shh moieties that can shield Ptc reduces with increasing conjugation ratio. This effect has been described theoretically (11) and may be incorporated in future model development. A simpler model without internalization gave an even poorer fit with experiment, as did models that did not incorporate acceleration of binding after initial binding of

a multivalent conjugate, indicating the likely importance of these processes to the bioactivity of the conjugates (data not shown). Both models with and without sterics fail to describe the peak amplitude in bioactivity of the 14:1 and 22:1 conjugates (Figure 6). In our modeling results, we noticed that Ptc receptor aggregation levels have a biphasic relationship with increasing Shh concentration (data not shown): Ptc aggregation peaks at an intermediate Shh concentration much like the experimental results in Figure 3. The biphasic relationship, as described in the literature (24), occurs because, at high Shh concentrations, HyA–Shh conjugates compete with one another for available receptors and will be typically bound to fewer receptors, resulting in a lower avidity. Therefore, a peak in bioactivity as a function of Shh concentration could be due to Ptc receptor aggregation resulting in cooperativity in Ptc signal transduction. Future experimental work detailing Ptc cooperativity in Shh signal transduction is needed to justify future incorporation of such effects into our simple models. Also in future work, the equivalent site assumption could be relaxed to devise a binding relationship that scales with valency. Again, future experimental Ptc binding studies with conjugates of various valency may justify the incorporation of this effect into our simple models.

This work has significant implications for the fields of drug delivery and biomaterials. The surprising finding that the potency of Shh grafted onto a linear polymer is increased significantly over freely soluble Shh could be very useful in the design and administration of therapeutics as a means to increase potency. In addition, significant research effort is currently directed to impart bioactivity to materials for biological and biomedical applications, and the data and modeling presented provide insight into how the forced clustering of proteins on a surface or in a 3D matrix may alter the potency of the added protein or change the effectiveness of a peptide sequence. For example, linear polymers modified with bioactive agents have been incorporated into hydrogel networks to make bioactive semi-interpenetrating networks for tissue engineering applications (34, 35). This research gives another form of modulation of added functionality in the solid state, as potency may be controllable by the both the amount of an agent added and its degree of substitution and spatial distribution.

ACKNOWLEDGMENT

This work was supported by LBNL LDRD 3668DS, by the Graduate Research and Education in Adaptive bio-Technology (GREAT) Training Program, UC Systemwide Biotechnology Research and Education Program 2005-280, and a Whitaker Foundation Graduate Fellowship.

Supporting Information Available: Details of the numerical kinetic model describing the signal pathway of Shh and the modifications to simulate the bioactivity effects of conjugated Shh are available. This material is available free of charge via the Internet at <http://pubs.acs.org>.

LITERATURE CITED

- (1) Kuhl, P. R., and Griffiths, L. G. (1996) Tethered epidermal growth factor as a paradigm for growth factor-induced stimulation from the solid phase. *Nat. Med.* 2, 1022–1027.
- (2) Moon, J. J., Lee, S. H., and West, J. L. (2007) Synthetic biomimetic hydrogels incorporated with Ephrin-A1 for therapeutic angiogenesis. *Biomacromolecules* 8, 42–49.
- (3) Seliktar, D., Zisch, A. H., Lutolf, M. P., Wrana, J. L., and Hubbell, J. A. (2004) MMP-2 sensitive, VEGF-bearing bioactive hydrogels for promotion of vascular healing. *J. Biomed. Mater. Res., Part A* 68A, 704–716.
- (4) Zisch, A. H., Lutolf, M. P., Ehrbar, M., Raebler, G. P., Rizzi, S. C., Davies, N., Schmokel, H., Bezuidenhout, D., Djonov, V., Zilla, P., and Hubbell, J. A. (2003) Cell-demanded release of VEGF from synthetic, biointeractive cell-ingrowth matrices for vascularized tissue growth. *FASEB J.* 17, 2260.
- (5) Ooya, T., and Yui, N. (2002) Multivalent interactions between biotin-polyrotaxane conjugates and streptavidin as a model of new targeting for transporters. *J. Controlled Release* 80, 219–228.
- (6) Segura, T., and Shea, L. D. (2002) Surface-tethered DNA complexes for enhanced gene delivery. *Bioconjugate Chem.* 13, 621–629.
- (7) Schaffer, D. V., and Lauffenburger, D. A. (1998) Optimization of cell surface binding enhances efficiency and specificity of molecular conjugate gene delivery. *J. Biol. Chem.* 273, 28004–28009.
- (8) Thoma, G., Duthaler, R. O., Magnani, J. L., and Patton, J. T. (2001) Nanomolar E-selectin inhibitors: 700-fold potentiation of affinity by multivalent ligand presentation. *J. Am. Chem. Soc.* 123, 10113–10114.
- (9) Pouyani, T., and Prestwich, G. D. (1994) Functionalized derivatives of hyaluronic-acid oligosaccharides - drug carriers and novel biomaterials. *Bioconjugate Chem.* 5, 339–347.
- (10) York, S. J., Arneson, L. S., Gregory, W. T., Dahms, N. M., and Kornfeld, S. (1999) The rate of internalization of the mannose 6-phosphate/insulin-like growth factor II receptor is enhanced by multivalent ligand binding. *J. Biol. Chem.* 274, 1164–1171.
- (11) Hlavacek, W. S., Posner, R. G., and Perelson, A. S. (1999) Steric effects on multivalent ligand-receptor binding: Exclusion of ligand sites by bound cell surface receptors. *Biophys. J.* 76, 3031–3043.
- (12) Hubble, J. (1999) A model of multivalent ligand-receptor equilibria which explains the effect of multivalent binding inhibitors. *Mol. Immunol.* 36, 13–18.
- (13) Muller, K. M., Arndt, K. M., and Pluckthun, A. (1998) Model and simulation of multivalent binding to fixed ligands. *Anal. Biochem.* 261, 149–158.
- (14) Huskens, J., Mulder, A., Auletta, T., Nijhuis, C. A., Ludden, M. J. W., and Reinhoudt, D. N. (2004) A model for describing the thermodynamics of multivalent host-guest interactions at interfaces. *J. Am. Chem. Soc.* 126, 6784–6797.
- (15) Lai, K., Kaspar, B. K., Gage, F. H., and Schaffer, D. V. (2003) Sonic hedgehog regulates adult neural progenitor proliferation in vitro and in vivo. *Nat. Neurosci.* 6, 21–27.
- (16) Pepinsky, R. B., Rayhorn, P., Day, E. S., Dergay, A., Williams, K. P., Galdes, A., Taylor, F. R., Boriack-Sjodin, P. A., and Garber, E. A. (2000) Mapping Sonic hedgehog-receptor interactions by steric interference. *J. Biol. Chem.* 275, 10995–11001.
- (17) Stile, R. A., and Healy, K. E. (2001) Thermo-responsive peptide-modified hydrogels for tissue regeneration. *Biomacromolecules* 2, 185–194.
- (18) Taylor, F. R., Wen, D. Y., Garber, E. A., Carmillo, A. N., Baker, D. P., Arduini, R. M., Williams, K. P., Weinreb, P. H., Rayhorn, P., Hronowski, X. P., Whitty, A., Day, E. S., Boriack-Sjodin, A., Shapiro, R. I., Galdes, A., and Pepinsky, R. B. (2001) Enhanced potency of human sonic hedgehog by hydrophobic modification. *Biochemistry* 40, 4359–4371.
- (19) Pepinsky, R. B., Zeng, C. H., Wen, D. Y., Rayhorn, P., Baker, D. P., Williams, K. P., Bixler, S. A., Ambrose, C. M., Garber, E. A., Miatkowski, K., Taylor, F. R., Wang, E. A., and Galdes, A. (1998) Identification of a palmitic acid-modified form of human Sonic hedgehog. *J. Biol. Chem.* 273, 14037–14045.
- (20) Pola, R., Ling, L. E., Silver, M., Corbley, M. J., Kearney, M., Pepinsky, R. B., Shapiro, R., Taylor, F. R., Baker, D. P., Asahara, T., and Isner, J. M. (2001) The morphogen Sonic hedgehog is an indirect angiogenic agent upregulating two families of angiogenic growth factors. *Nat. Med.* 7, 706–711.
- (21) Saha, K., and Schaffer, D. V. (2006) Signal dynamics in Sonic hedgehog tissue patterning. *Development* 133, 889–900.
- (22) Lai, K., Robertson, M. J., and Schaffer, D. V. (2004) The Sonic hedgehog signaling system as a bistable genetic switch. *Biophys. J.* 86, 2748–2757.

- (23) Perelson, A. S. (1981) Receptor clustering on a cell-surface 0.3. theory of receptor cross-linking by multivalent ligands - description by ligand states. *Math. Biosci.* 53, 1–39.
- (24) Lauffenburger, D. A., and Linderman, J. J. (1993) Receptors: Models for Binding, Trafficking, and Signaling. Oxford University Press, New York.
- (25) Vercruyse, K. P., Marecak, D. M., Marecek, J. F., and Prestwich, G. D. (1997) Synthesis and in vitro degradation of new polyvalent hydrazide cross-linked hydrogels of hyaluronic acid. *Bioconjugate Chem.* 8, 686–694.
- (26) Bulpitt, P., and Aeschlimann, D. (1999) New strategy for chemical modification of hyaluronic acid: Preparation of functionalized derivatives and their use in the formation of novel biocompatible hydrogels. *J. Biomed. Mater. Res.* 47, 152–169.
- (27) Stile, R. A., Barber, T. A., Castner, D. G., and Healy, K. E. (2002) Sequential robust design methodology and X-ray photoelectron spectroscopy to analyze the grafting of hyaluronic acid to glass substrates. *J. Biomed. Mater. Res.* 61, 391–398.
- (28) Shu, X. Z., Liu, Y. C., Luo, Y., Roberts, M. C., and Prestwich, G. D. (2002) Disulfide cross-linked hyaluronan hydrogels. *Biomacromolecules* 3, 1304–1311.
- (29) Luo, Y., Ziebell, M. R., and Prestwich, G. D. (2000) A hyaluronic acid-taxol antitumor bioconjugate targeted to cancer cells. *Biomacromolecules* 1, 208–218.
- (30) Luo, Y., and Prestwich, G. D. (1999) Synthesis and selective cytotoxicity of a hyaluronic acid-antitumor bioconjugate. *Bioconjugate Chem.* 10, 755–763.
- (31) Feng, J., White, B., Tyurina, O. V., Guner, B., Larson, T., Lee, H. Y., Karlstrom, R. O., and Kohtz, J. D. (2004) Synergistic and antagonistic roles of the Sonic hedgehog N- and C-terminal lipids. *Development* 131, 4357–4370.
- (32) Torroja, C., Gorfinkiel, N., and Guerrero, I. (2004) Patched controls the Hedgehog gradient by endocytosis in a dynamin-dependent manner, but this internalization does not play a major role in signal transduction. *Development* 131, 2395–2408.
- (33) Incardona, J. P., Lee, J. H., Robertson, C. P., Enga, K., Kapur, R. P., and Roelink, H. (2000) Receptor-mediated endocytosis of soluble and membrane-tethered Sonic hedgehog by Patched-1. *Proc. Natl. Acad. Sci. U.S.A.* 97, 12044–12049.
- (34) Stile, R. A., Chung, E., Burghardt, W. R., and Healy, K. E. (2004) Poly(N-isopropylacrylamide)-based semi-interpenetrating polymer networks for tissue engineering applications. Effects of linear poly(acrylic acid) chains on rheology. *J. Biomater. Sci.-Polym. Ed.* 15, 865–878.
- (35) Chung, E. H., Gilbert, M., Viridi, A. S., Sena, K., Sumner, D. R., and Healy, K. E. (2006) Biomimetic artificial ECMs stimulate bone regeneration. *J. Biomed. Mater. Res., Part A* 79A, 815–826.

BC700265K